Strength of Materials and Elasticity Approach to Stiffness of Fibrous Composites Using the Concept of Interphase

E. Sideridis, G. A. Papadopoulos, E. Kyriazi

Department of Mechanics, National Technical University of Athens, 5 Heroes of Polytechnion Ave., GR-157 73, Zographou, Athens, Greece

ABSTRACT: A strength of materials and elasticity approach was used in this study to determine the stiffness of fiber-reinforced composites, by taking into account the concept of boundary interphase. Theoretical expressions for longitudinal transverse and shear moduli, as well as for longitudinal Poisson's ratio, were derived by use of this model. Results derived from these expressions were compared with others, to observe the discrepancies and evaluate their validity.© 2005 Wiley Periodicals, Inc. J Appl Polym Sci 95: 1578–1588, 2005

Key words: strength; shear; modulus; elasticity; modeling

INTRODUCTION

The division of micromechanics stiffness evaluation efforts into a strength of materials approach and an elasticity approach, with its many subapproaches, is rather arbitrary.[1] Chamis and Sendeckyj[2] divide micromechanics stiffness approaches into many more classes: netting analysis, strength of material approaches, self-consistent models, variational techniques using energy bounding principles, exact solutions, statistical approaches, discrete element methods, semiempirical approaches, and microstructure theories. All the approaches have the common objective of the prediction of composite stiffness. All except the first two approaches use some or all of the principles of elasticity theory to varying degrees so are here classed as elasticity approaches. This simplifying and arbitrary division is useful because the objective here is to merely become acquainted with advanced micromechanics theories after the basic concepts have been introduced by use of strength of materials type reasoning.

The variational energy principles of classical elasticity theory were used to determine upper and lower bounds on the moduli of unidirectional fiber-reinforced composites. However, that approach generally leads to bounds that may not be sufficiently close for practical use.

A large critique on theories predicting thermoelastic properties of fibrous composites was presented by Chamis and Sendeckyj.[2] Also, a large survey, the purpose of which is to review the analysis of composite materials from the applied mechanics and engineering science perspective, was carried out by Hashin.[3]

The majority of the models introduced for explaining the mechanical behavior of composites have a common characteristic of considering the fiber–matrix interface as a perfect mathematical surface. However, in reality the situation is much different because of the roughness of the filler.

Thus, around an inclusion embedded in a matrix a rather complex situation develops, consisting of areas of imperfect bonding, permanent stresses resulting from shrinkage, and high-stress gradients or even stress singularities, attributed to the geometry of the inclusions, voids, and microcracks, for example.

Moreover, the interaction of the fiber with the matrix is usually a much more complicated procedure than a simple mechanical effect. The presence of a fiber actually restricts the segmental and molecular mobility of the polymeric matrix, as absorption interaction in polymer surface layers into fibers occurs. It is then obvious that, under these conditions, the quality of adhesion can hardly be quantified and a more thorough investigation by assuming the existence of a third phase between matrix and fiber is necessary.

Examples of three-phase work dealing with fiber composites have been given by Theocaris et al.[4] Mikata and Taya,[5] Pagano and Tandon,[6] Benveniste et al.,[7] Steif and Dollar,[8] and Achenbach and Zhu.[9]

In this article, by the aid of a strength of materials approach and an elasticity approach, an investigation was carried out to determine theoretical expressions for longitudinal, transverse, and shear moduli, as well as for longitudinal Poisson's ratio using the recently developed interphase model.
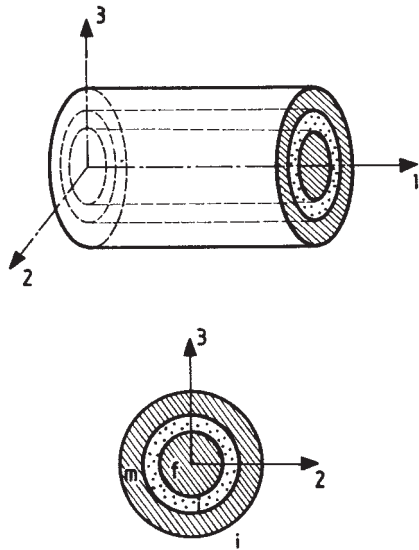
Figure 1 (a) Schematic depiction of the model used for the representative volume element of a unidirectional fiber composite; (b) its cross-sectional area.

STRENGTH OF MATERIALS APPROACH TO STIFFNESS

The main feature of the strength of materials approach is that certain simplifying assumptions are made regarding the mechanical behavior of a composite material. The most prominent assumption is that the strains in the fiber direction of a unidirectional fibrous composite are the same in the fibers, in the interphase, and in the matrix, as shown in Figure 1. Because the strains are the same in the three phases, then it is obvious that sections normal to the 1-axis that were plane before being stressed remain plane after stressing. We shall derive, on that basis, the strength of materials expressions for the apparent orthotropic moduli of a unidirectionally reinforced fibrous composite material.

Longitudinal elastic modulus E_1

The longitudinal elastic modulus of the composite in the 1-direction, that is, in the fiber direction can be determined as follows. From Figure 2 the strain ε_1 is given as

$$\varepsilon_1 = \Delta L / L \tag{1}$$

where ε_1 applies for fibers, interphase, and matrix according to the basic assumption. When the three constituent materials behave elastically, the stresses are

$$\sigma_f = E_f \varepsilon_1 \quad \sigma_i = E_i \varepsilon_1 \quad \sigma_m = E_m \varepsilon_1 \tag{2a,b,c}$$

The average stress σ_1 acts on a cross-sectional area A, σ_f acts on the cross-sectional area of the fibers A_f, σ_i acts on the cross-sectional area of the interphase A_i, and σ_m acts on the cross-sectional area of the matrix A_m. Thus, the resultant force on the element of composite material is

$$P = \sigma_1 A = \sigma_f A_f + \sigma_i A_i + \sigma_m A_m \tag{3}$$

By substitution of eq. (2) into eq. (3) and recognition that

$$\sigma_1 = E_1 \varepsilon_1 \tag{4}$$

apparently

$$E_1 = E_f(A_f/A) + E_i(A_i/A) + E_m(A_m/A) \tag{5}$$

However, the volume fraction of the three phases can be written as

$$v_f = A_f/A \quad v_i = A_i/A \quad v_m = A_m/A \tag{6a,b,c}$$

Thus

$$E_1 = E_f v_f + E_i v_i + E_m v_m \tag{7}$$

which is a "refined" law of mixtures expression for the apparent Young's modulus in the direction of the fibers.

Transverse elastic modulus E_2

The apparent Young's modulus E_2, in the direction transverse to the fibers, can be determined assuming that the same transverse stress σ_2 is to be applied to fiber, interphase, and matrix as in Figure 3. The strains in the three phases are thus

$$\varepsilon_f = \sigma_2/E_f \quad \varepsilon_i = \sigma_2 E_i \quad \varepsilon_m = \sigma_2/E_m \tag{8a,b,c}$$

The transverse dimension over which, on the average, ε_f acts is approximately $v_f W$, whereas ε_i acts on $v_i W$
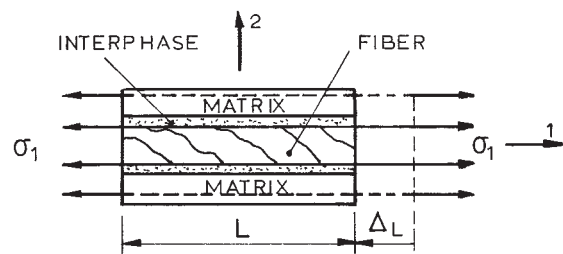

Figure 2 Representative volume element loaded in 1-direction for E_1.
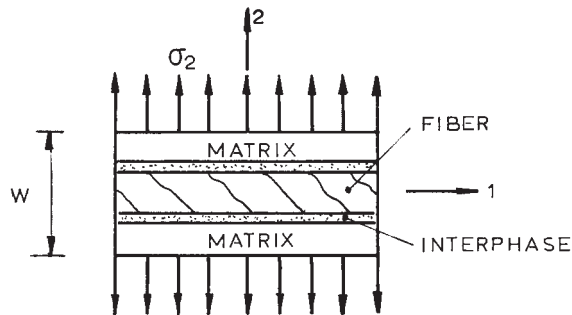
Figure 3 Representative volume element loaded in 2-direction for E_2.

and ε_m acts on $v_m W$. Thus, the total transverse deformation is

$$\varepsilon_2 W = v_f W \varepsilon_f + v_i W \varepsilon_i + v_m W \varepsilon_m \qquad (9)$$

or

$$\varepsilon_2 = v_f \varepsilon_f + v_i \varepsilon_i + v_m \varepsilon_m \qquad (10)$$

which becomes, upon substitution of eq. (8),

$$\varepsilon_2 = v_f(\sigma_2/E_f) + v_i(\sigma_2/E_i) + v_m(\sigma_2/E_m) \qquad (11)$$

but

$$\sigma_2 = E_2 \varepsilon_2 = E_2[v_f(\sigma_2/E_f) + v_i(\sigma_2/E_i) + v_m(\sigma_2/E_m)] \qquad (12)$$

whereupon

$$E_2 = E_f E_i E_m / (E_i E_m v_f + E_f E_m v_i + E_f E_i v_m) \qquad (13)$$

Longitudinal Poisson's ratio v_{12}

The so-called major Poisson's ratio v_{12} can be obtained by use of an approach similar to the analysis for E_1. The major Poisson's ratio is defined as

$$v_{12} = -\varepsilon_2/\varepsilon_1 \qquad (14)$$

for the stress state $\sigma_1 = \sigma$ and all other stresses are zero. The deformations are depicted in Figure 4. The transverse deformation ΔW is

$$\Delta W = -W\varepsilon_2 = W v_{12}\varepsilon_1 \qquad (15)$$

but is also

$$\Delta W = \Delta_f + \Delta_i + \Delta_m \qquad (16)$$
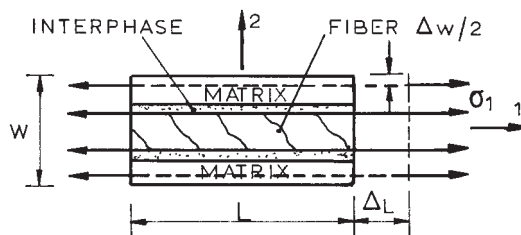

Figure 4 Representative volume element loaded in 1-direction for v_{12}.

In the manner of the analysis for the transverse Young's modulus E_2, the deformations Δ_f, Δ_i, and Δ_m are approximately

$$\Delta_f = W v_f v_f \varepsilon_1 \quad \Delta_i = W v_i v_i \varepsilon_1 \quad \Delta_m = W v_m v_m \varepsilon_1$$
$$(17\text{a,b,c})$$

Thus upon combination of eqs. (15)–(17), division by $\varepsilon_1 W$ yields

$$v_{12} = v_f v_f + v_i v_i + v_m v_m \qquad (18)$$

which is a "refined" law of mixtures for the major Poisson's ratio.

In-plane shear modulus G_{12}

The in-plane shear modulus G_{12} is determined by assuming that the shearing stresses on the fiber, the interphase, and the matrix are the same. The loading is shown in Figure 5. By virtue of the basic assumption

$$\gamma_f = \tau/G_f \quad \gamma_i = \tau/G_i \quad \gamma_m = \tau/G_m \qquad (19)$$

The nonlinear shear stress–shear strain behavior typical of fiber-reinforced composites is ignored (i.e., the behavior is regarded as linear).

On a microscopic scale, the deformations are shown in Figure 6. The total shearing deformation is defined as
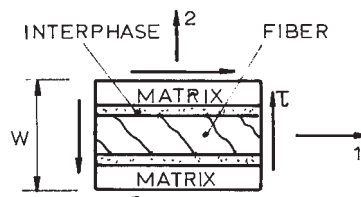
$$\Delta = \gamma W \qquad (20)$$

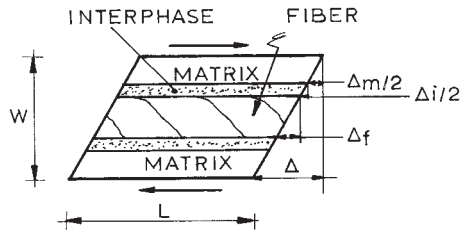**Figure 5** Representative volume element loaded in shear for G_{12}.

Figure 6 Shear deformation of a representative volume element.

and is made up of, approximately

$$\Delta_f = v_f W \gamma_f \quad \Delta_i = v_i W \gamma_i \quad \Delta_m = v_m W \gamma_m \quad \text{(21a,b,c)}$$

Then given that $\Delta = \Delta_f + \Delta_i + \Delta_m$, division by W yields

$$\gamma = v_f \gamma_f + v_i \gamma_i + v_m \gamma_m \tag{22}$$

or upon substitution of eq. (19) and realization that

$$\gamma = \tau / G_{12} \tag{23}$$

Equation (22) can be written as

$$\tau / G_{12} = v_f(\tau/G_f) + v_i(\tau/G_i) + v_m(\tau/G_m) \tag{24}$$

Finally

$$G_{12} = G_f G_i G_m / (G_i G_m v_f + G_f G_m v_i + G_f G_i v_m) \tag{25}$$

which is the same type of expression as was obtained for the transverse Young's modulus E_2.

Summarizing, it can be said that the foregoing are but examples of the types of strength of materials approaches that can be used. Other assumptions of physical behavior lead to different expressions for the four moduli of a unidirectional fiber-reinforced composite. For example, Ekvall[10] obtained a modification of the expressions for E_1 and E_2 in which the triaxial stress state in the matrix, arising from fiber restraint, is accounted for. Thus eqs. (7) and (13) can be written as

$$E_1 = E_f v_f + E_i v_i + E'_m v_m \tag{26}$$

$$E_2 = E_f E_i E'_m / [E_i E'_m v_f + E_f E'_m v_i + E_f E_i v_m(1 - v_m^2)] \tag{27}$$

where

$$E'_m = E_m / (1 - 2v_m^2) \tag{28}$$

ELASTICITY APPROACH TO STIFFNESS

Bounding techniques of elasticity

Paul[11] was apparently the first to use the variational (bounding) techniques of linear elasticity to examine the bounds on the moduli of multiphase materials. His work was directed toward analysis of the elastic moduli of alloyed metals rather than toward fibrous composites. Accordingly, the treatment is for an isotropic composite material made of isotropic constituents. The modulus of the basic matrix is E_m, the modulus of the filler material is E_f, the modulus of the interphase is E_i, whereas the modulus of the composite material is E. The volume fractions of the constituents are v_f, v_i, and v_m such that

$$v_f + v_i + v_m = 1 \tag{29}$$

Obviously, any relationship for the composite modulus E must yield $E = E_m$ for $v_m = 1$ and $E = E_f$ for $v_f = 1$ because in these cases no interphase should exist (i.e., $v_i = 0$).

Lower bound on apparent Young's modulus

The basis for the determination of a lower bound on the apparent Young's modulus is application of the minimum complementary energy which can be stated as: Let the tractions (forces and moments) be specified over the surface of a body. Let σ_x^0, σ_y^0, σ_z^0, τ_{xy}^0, τ_{yz}^0, τ_{zx}^0 be a state of stress that satisfies the stress equations of equilibrium and the specified boundary conditions. Let U^0 be the strain energy for the stress state σ_x^0, σ_y^0, σ_z^0, τ_{xy}^0, τ_{yz}^0, τ_{zx}^0 given by use of the stress–strain relationships

$$\sigma_x = [\nu E / (1 + \nu)(1 - 2\nu)](\varepsilon_x + \varepsilon_y + \varepsilon_z) + [E/(1 + \nu)]\varepsilon_x$$
$$\vdots$$
$$\tau_{xy} = G\gamma_{xy} = [E/2(1 + \nu)]\gamma_{xy} \tag{30}$$

and the expression for the strain energy

$$U = (1/2) \int_V (\sigma_x \varepsilon_x + \sigma_y \varepsilon_y + \sigma_z \varepsilon_z + \tau_{xy}\gamma_{xy} + \tau_{yz}\gamma_{yz} + \tau_{zx}\gamma_{zx}) \, dV \tag{31}$$

Then, the actual strain energy U in the body attributed to the specified loads cannot exceed U^0, that is,

$$U \le U^0 \tag{32}$$

To find a lower bound on the apparent Young's modulus E, load the basic uniaxial test specimen with

normal stress on the ends. The internal stress field that satisfies this loading and the stress equations of equilibrium is

$$\sigma_x^0 = \sigma \quad \sigma_y^0 = \sigma_z^0 = \tau_{xy}^0 = \tau_{yz}^0 = \tau_{zx}^0 = 0 \qquad (33)$$

The strain energy for the stresses in eq. (33) is

$$U^0 = \frac{1}{2} \int_V \frac{(\sigma_x^0)^2}{E} \, dV = \frac{\sigma^2}{2} \int_V \frac{dV}{E} \qquad (34)$$

However, E is obviously nonconstant over the volume because the filler has modulus E_f over volume $v_f V$, the interphase has modulus E_i over volume χV_i, and the matrix has modulus E_m over volume $v_m V$, where V is the total volume. Thus

$$\int_V \frac{dV}{E} = \int_{V_f} \frac{dV}{E_f} + \int_{V_i} \frac{dV}{E_i} + \int_{V_m} \frac{dV}{E_m} \qquad (35)$$

or

$$\int_V \frac{dV}{E} = \frac{v_f V}{E_f} + \frac{v_i V}{E_i} + \frac{v_m V}{E_m} \qquad (36)$$

From eqs. (34) and (36) we obtain

$$U^0 = \frac{\sigma^2}{2} \left[\frac{v_f}{E_f} + \frac{v_i}{E_i} + \frac{v_m}{E_m} \right] V \qquad (37)$$

However, by virtue of the inequality $U \leq U^0$ and because $U = \frac{1}{2}[\sigma^2/E)V]$, the above relationship can be written as

$$\frac{1}{2} \frac{\sigma^2}{E} V \leq \frac{\sigma^2}{2} \left[\frac{v_f}{E_f} + \frac{v_i}{E_i} + \frac{v_m}{E_m} \right] V \qquad (38)$$

or

$$\frac{1}{E} \leq \frac{v_f}{E_f} + \frac{v_i}{E_i} + \frac{v_m}{E_m} \qquad (39)$$

and finally

$$E \geq \frac{E_f E_i E_m}{E_i E_m v_f + E_f E_m v_i + E_f E_i v_m} \qquad (40)$$

which is a lower bound on the apparent Young's modulus E, of the composite material in terms of the moduli and volume fractions of the three phases. This bound coincides with the value for the modulus transverse to fibers by the strength of materials approach.

Upper bound on apparent Young's modulus

The basis for the determination of an upper bound on the apparent Young's modulus is application of the principle of minimum potential energy, which can be stated as: Let the displacements be specified over the surface of the body except where the corresponding traction is zero. Let $\varepsilon_x^*, \varepsilon_y^*, \varepsilon_z^*, \gamma_{xy}^*, \gamma_{yz}^*, \gamma_{zx}^*$ be any compatible state of strain that satisfies the specific displacement boundary conditions. Let U^* be the strain energy of the strain state $\varepsilon_x^*, \varepsilon_y^*, \varepsilon_z^*, \gamma_{xy}^*, \gamma_{yz}^*, \gamma_{zx}^*$ by use of the stress–strain relationships of eq. (30), and the expression for the strain energy given by eq. (31).

Then, the actual strain energy U in the body arising from the specified displacements cannot exceed U^*, that is,

$$U \leq U^* \qquad (41)$$

To find an upper bound on the apparent Young's modulus E, subject the basic uniaxial test specimen to an elongation eL, where e is the average strain and L is the specimen length. The internal strain field that corresponds to the average strain at the boundaries of the specimen is

$$\varepsilon_x^* = \varepsilon \quad \varepsilon_y^* = \varepsilon_x^* = -\nu\varepsilon \quad \gamma_{xy}^* = \gamma_{yz}^* = \gamma_{zx}^* = 0 \quad (42)$$

where ν is the apparent Poisson's ratio of the composite. Then by using the stress–strain relationships of eq. (30), the stresses in the three phases for the given strain field are

$$\sigma_{x,f}^* = \frac{1 - \nu_f - 2\nu_f \nu}{1 - \nu_f - 2\nu_f^2} E_f \varepsilon \quad \sigma_{y,f}^* = \sigma_{z,f}^* = \frac{\nu_f - \nu}{1 - \nu_f - 2\nu_f^2} E_f \varepsilon$$

$$\tau_{xy,f}^* = \tau_{yz,f}^* = \tau_{zx,f}^* = 0 \quad (43)$$

for the filler

$$\sigma_{x,i}^* = \frac{1 - \nu_i - 2\nu_i \nu}{1 - \nu_i - 2\nu_i^2} E_i \varepsilon \quad \sigma_{y,i}^* = \sigma_{z,i}^* = \frac{\nu_i - \nu}{1 - \nu_i - 2\nu_i^2} E_i \varepsilon$$

$$\tau_{xy,i}^* = \tau_{yz,i}^* = \tau_{zx,i}^* = 0 \quad (44)$$

for the interphase

$$\sigma_{x,m}^* = \frac{1 - \nu_m - 2\nu_m \nu}{1 - \nu_m - 2\nu_m^2} E_m \varepsilon$$

$$\sigma_{y,m}^* = \sigma_{z,m}^* = \frac{\nu_m - \nu}{1 - \nu_m - 2\nu_m^2} E_i \varepsilon$$

$$\tau_{xy,m}^* = \tau_{yz,m}^* = \tau_{zx,m}^* = 0 \quad (45)$$

for the matrix.

The strain energy in the composite material is obtained by substituting the strains from eqs. (42) and

the stresses from eqs. (43)–(45) in the strain energy, eq. (30)

$$U^* = \frac{\varepsilon^2}{2} \int_{V_f} \frac{1 - \nu_f - 4\nu_f\nu + 2\nu^2}{1 - \nu_f - 2\nu_f^2} E_f \, dV$$

$$+ \frac{\varepsilon^2}{2} \int_{V_i} \frac{1 - \nu_i - 4\nu_i\nu + 2\nu^2}{1 - \nu_i - 2\nu_i^2} E_i \, dV$$

$$+ \frac{\varepsilon^2}{2} \int_{V_m} \frac{1 - \nu_m - 4\nu_m\nu + 2\nu^2}{1 - \nu_m - 2\nu_m^2} E_m \, dV \quad (46)$$

or

$$U^* = \frac{\varepsilon^2}{2} \left(\frac{1 - \nu_f - 4\nu_f\nu + 2\nu^2}{1 - \nu_f - 2\nu_f^2} E_f\upsilon_f \right.$$

$$+ \frac{1 - \nu_i - 4\nu_i\nu + 2\nu^2}{1 - \nu_i - 2\nu_i^2} E_i\upsilon_i$$

$$\left. + \frac{1 - \nu_m - 4\nu_m\nu + 2\nu^2}{1 - \nu_m - 2\nu_m^2} E_m\upsilon_m \right) V \quad (47)$$

However, by virtue of the inequality $U \le U^*$ and the definition $U = \frac{1}{2}E\varepsilon^2 V$, after some algebra we find the upper bound as

$$E \le \frac{1 - \nu_f - 4\nu_f\nu + 2\nu^2}{1 - \nu_f - 2\nu_f^2} E_f\upsilon_f$$

$$+ \frac{1 - \nu_i - 4\nu_i\nu + 2\nu^2}{1 - \nu_i - 2\nu_i^2} E_i\upsilon_i$$

$$+ \frac{1 - \nu_m - 4\nu_m\nu + 2\nu^2}{1 - \nu_m - 2\nu_m^2} E_m\upsilon_m \quad (48)$$

The value of the Poisson's ratio ν for the composite is unknown at this stage of the analysis, so the upper bound on E is nonspecific. In accordance with the principle of minimum potential energy the expression for the strain energy U^* must be minimized with respect to the unspecified constant ν to specify the bound on E. This procedure consists of determining where

$$\frac{\partial U^*}{\partial \nu} = 0 \quad (49)$$

and at the same time

$$\frac{\partial^2 U^*}{\partial \nu^2} > 0 \quad (50)$$

First

$$\frac{\partial U^*}{\partial \nu} = \frac{\varepsilon^2 V}{2} \left(\frac{-4\nu_f + 4\nu}{1 - \nu_f - 2\nu_f^2} E_f\upsilon_f + \frac{-4\nu_i + 4\nu}{1 - \nu_i - 2\nu_i^2} E_i\upsilon_i \right.$$

$$\left. + \frac{-4\nu_m + 4\nu}{1 - \nu_m - 2\nu_m^2} E_m\upsilon_m \right) = 0 \quad (51)$$

which is zero when

$$\nu = \frac{\begin{array}{l}(1 - \nu_f - 2\nu_f^2)E_f\upsilon_f\nu_f + (1 - \nu_i - 2\nu_i^2) \\ E_i\upsilon_i\nu_i + (1 - \nu_m - 2\nu_m^2)E_m\upsilon_m\nu_m\end{array}}{\begin{array}{l}(1 - \nu_f - 2\nu_f^2)E_f\upsilon_f + (1 - \nu_i - 2\nu_i^2) \\ \times E_i\upsilon_i + (1 - \nu_m - 2\nu_m^2)E_m\upsilon_m\end{array}} \quad (52)$$

The second derivative of U^* is

$$\frac{\partial^2 U^*}{\partial \nu^2} = \frac{\varepsilon^2 V}{2} \left(\frac{4E_f\upsilon_f}{1 - \nu_f - 2\nu_f^2} + \frac{4E_i\upsilon_i}{1 - \nu_i - 2\nu_i^2} \right.$$

$$\left. + \frac{4E_m\upsilon_m}{1 - \nu_m - 2\nu_m^2} \right) \quad (53)$$

Given that $\nu_f < \frac{1}{2}$, $\nu_i < \frac{1}{2}$, $\nu_m < \frac{1}{2}$ (the usual limit on Poisson's ratio for an isotropic material) the value of $\partial^2 U^*/\partial \nu^2$ is seen to be always positive, given that the terms $1 - \nu_f - 2\nu_f^2$, $1 - \nu_i - 2\nu_i^2$, and $1 - \nu_m - 2\nu_m^2$ are always positive when $\nu < \frac{1}{2}$.

Finally, because $\partial^2 U^*/\partial \nu^2$ is always positive, the value of U^* when eq. (52) is used, corresponding to a minimum, maximum, or inflection point on the curve for U^* as a function of ν, is proved to be a minimum.

The value of Poisson's ratio ν for the composite has been derived explicitly as in eq. (52). Thus, the explicit upper bound on E can be obtained by substituting this expression for ν in the expression for the upper bound on E in terms of ν given by eq. (48). For the special case in which $\nu_f = \nu_i = \nu_m$, eq. (52) reduces to $\nu = \nu_f = \nu_i = \nu_m$, so the upper bound on E reduces to

$$E \le E_f\upsilon_f + E_i\upsilon_i + E_m\upsilon_m \quad (54)$$

which is the value of the apparent Young's modulus E_1, in the fiber direction of a fibrous composite derived by a strength of materials approach. Thus the expression for E_1 is an upper bound on the actual E_1. In addition, the strength of materials solution obviously includes an implicit equality of the Poisson's ratios of the constituent materials.

THE INTERPHASE MODEL

Let us consider the model for the representative volume element (RVE) for a fiber-reinforced composite presented in Figure 1(b). The composite consists of three different materials. The fiber is surrounded by

the interphase and this, in turn, is surrounded by the matrix.

If we denote by r_f, r_i, and r_m the outer radii of the fiber, the interphase, and the matrix circular sections, respectively, then the fractions of the respective phases are given by

$$v_f = \frac{r_f^2}{r_m^2} \quad v_i = \frac{r_i^2 - r_f^2}{r_m^2} \quad v_m = \frac{r_m^2 - r_i^2}{r_m^2} \quad (55)$$

with

$$v_f + v_i + v_m = 1$$

where v denotes the volume fraction and the indices f, i, and m correspond to the fiber, interphase, and matrix, respectively.

As the fiber-volume fraction is increased, the proportion of macromolecules, characterized by a reduced mobility, is also increased. This is equivalent with an increase in interphase volume fraction and leads to the conclusion, stated in Lipatov,[12] that is a relation between Δc_p, expressing the sudden change in specific heat at the glass-transition region of the substances, and the interphase volume fraction v_f. This relation for fiber composites is expressed by

$$\left(\frac{r_f + \Delta r}{r_f}\right)^2 - 1 = \frac{\lambda v_f}{1 - v_f} \quad (56)$$

where Δr is the thickness of interphase and the parameter λ is given by[12]

$$\lambda = 1 - \frac{\Delta c_p^f}{\Delta c_p^0} \quad (57)$$

in which Δc_p^f and Δc_p^0 are the sudden changes of the specific heat for the filled and the unfilled polymer, respectively, at their respective glass-transition regions.

Then, by measuring with the aid of thermal analysis (DSC measurements) the specific heat jumps (Δc_p's) at the glass transition of a fiber composite and its respective polymer made exclusively from the matrix material, the weight factor λ may be evaluated and the thickness of the interphase can be determined from the volume fraction of the fibers.

To evaluate the interphase elastic modulus $E_i(r)$, shear modulus $G_i(r)$ and Poisson's ratio $v_i(r)$ modes of variation were considered. Generally, for the above-mentioned elastic constants $M_i(r)$, a polynomial variation of the form

$$M_i(r) = f(r) = Ar^n + Br^{n-1} + Cr^{n-2} + \cdots \quad (58)$$

with $r_f < r < r_i$ can be considered. The constants A, B, C, $\cdots$ can be evaluated from the boundary conditions:

$$\text{At} \quad r = r_i \rightarrow M_i(r) = M_m$$

$$\text{At} \quad r = r_f \rightarrow M_i(r) = kM_f \quad (59)$$

together with the condition $dM_i(r)/dr = 0$ wherever we have an extremum. However, to evaluate the maximum influence of the interphase, the coefficient k is taken as $k = 1$, thus assuming that the interphase constants $M_i(r)$ are equal to M_f at $r = r_f$. In this study the parabolic variation of $M_i(r)$ is considered. From eq. (58) for $n = 2$ we have

$$M_i(r) = Ar^2 + Br + C \quad (60)$$

and the boundary conditions [eq. (59)] with $dM_i(r)/dr = 0$ at $r = r_i$. By applying these conditions we find

$$M_i(r) = \frac{M_f - M_m}{(r_i - r_f)^2} r^2 - \frac{2(M_f - M_m)r_i}{(r_i - r_f)^2} r$$

$$+ \frac{M_f r_i^2 + M_m r_f^2 - 2M_m r_f r_i}{(r_i - r_f)^2} \quad (61)$$

The average values for the interphase constants can be calculated by

$$\overline{M}_i = \frac{1}{v_i} \int_{r_f}^{r_i} M_i(r) \, dv = \frac{2v_f}{v_i r_f^2} \int_{r_f}^{r_i} M_i(r) \, dr \quad (62)$$

The elastic constants of fiber and matrix material used in the theoretical calculations are as follows:

$$E_f = 72 \text{ GPa} \quad E_m = 3.5 \text{ GPa} \quad v_f = 0.20 \quad v_m = 0.36$$

EXPERIMENTAL WORK

The material that was used in this study was Perma-Glas XEB5/1 of Permali Gloucester Ltd. (Gloucester, UK), which is a unidirectional glass fiber–epoxy resin laminate fabricated by using filament-winding methods in the form of about 5.8-mm-thick sheets. The glass-fiber–epoxy sheets contained about 80%, by weight, glass fibers, embedded in an Araldite MY 750/HT 972 (Ciba-Geigy, Leeds, UK) epoxy resin. This is based on the diglycidyl ether of bisphenol A and was cured using an aromatic amine hardener. The volume fraction v_f was determined, as customary, by igniting samples of the composite and weighing the residue, which gave the weight fraction of glass as 79.6 $\pm$ 0.28%. This and the measured values of the relative densities of PermaGlas ($\rho_f = 2.55$) and of the epoxy matrix ($\rho_m = 1.20$) gave the value $v_f = 0.65$. The fibers had a diameter of 12×10^{-6} m.
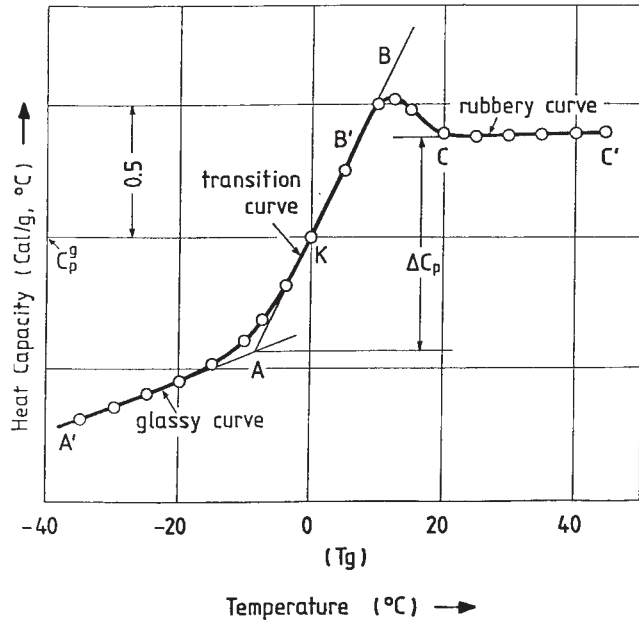
Figure 7 Typical DSC trace for the specific heat jump Δc_p at the glass-transition region of E-glass fiber epoxy composite.

On the other hand, chip specimens with a 4-mm diameter and thicknesses varying between 1 and 1.5 mm, made of the fiber composite and of the matrix material, were tested on a differential scanning calorimetry (DSC) thermal analyzer at the zone of the glass-transition temperature to determine the specific heat values. The values of the weight factor λ were derived from the values of Δc_p^f and Δc_p^0 measured from the $\Delta c_p = f(T)$ diagrams, where T denotes the temperature. The values of λ determined from these DSC tests allowed the evaluation of the thickness Δr the interphase according to eqs. (56) and (57).

RESULTS AND DISCUSSION

Figure 7 presents the typical DSC trace for the variation of the specific heat versus the temperature. A jump Δc_p can be seen in the specific heat at the glass-transition region. The values of the factor λ in eq. (56) were derived from the values of Δc_p^f and Δc_p^0 measured from the $\Delta c_p = f(T)$ diagram of this figure. The values of λ, determined from these DSC tests, allowed the evaluation of the thickness Δr of the interphase for the composite.

Figure 8 presents the variation of Δc_p values at the glass-transition region, the factor λ, as well as the values v_i and v_m versus the fiber volume fraction v_f for the E-glass fiber–reinforced composites.

It has been shown[13] that for unidirectional glass fiber–reinforced epoxy composites, a simple relation between the volume fraction of the interphase v_i and fiber volume fraction v_f holds:

$$v_i = C v_f^2 \qquad (63)$$

with the constant C found to be 0.123.

From this figure it can be observed that the interphase volume fraction v_i increases with increasing fiber content v_f. On the contrary, the matrix volume fraction v_m decreases, as expected, because it can be said that the naturally developed interphase constitutes an alteration of the matrix. It can also be seen that the change in the specific heat Δc_p decreases when $0 \le v_f \le 0.10$ when the fiber volume fraction increases, then increases slightly when $0.10 \le v_f \le 0.40$, and finally seems to be constant for $v_f > 0.40$.

Figure 9 shows the variation of the elastic modulus in the direction of fibers, E_1, as calculated through eq. (7) normalized by E_m. It represents a linear variation of the apparent Young modulus E_1 from E_m to E_f. This variation is analogous to that given by the law of mixtures.

The values obtained from eq. (7), however, are superior to those given by the mixtures law because, as calculated by eqs. (61) and (62), the interphase modulus E_i is greater than the matrix modulus E_m and because $v_i = 1 - v_f - v_m$. Thus

$$E_1 = E_f v_f + E_m v_m - E_i(v_f + v_m) + E_i$$

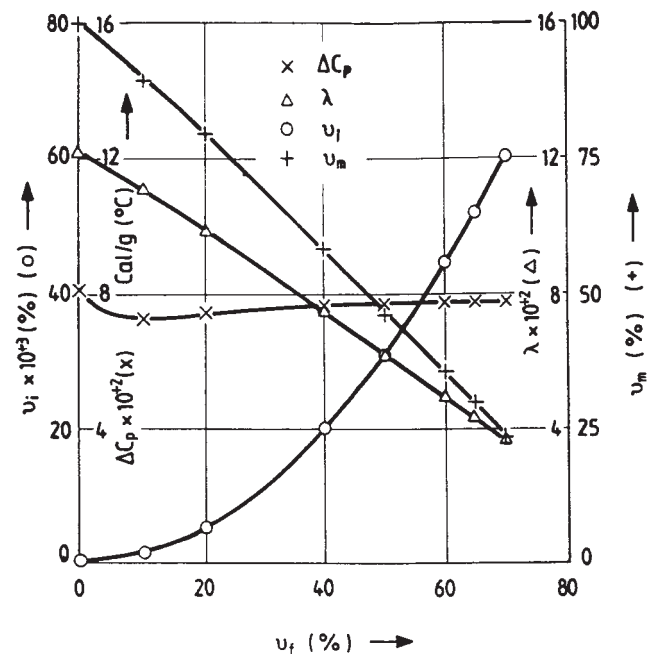which is greater than that given by the mixture law, $E_1 = E_f v_f + E_m v_m$.

Figure 8 Variation of the specific heat jumps Δc_p at the glass-transition temperature of E-glass fiber epoxy composite and the values of the λ factor and the interphase volume fraction v_i versus fiber content v_f.
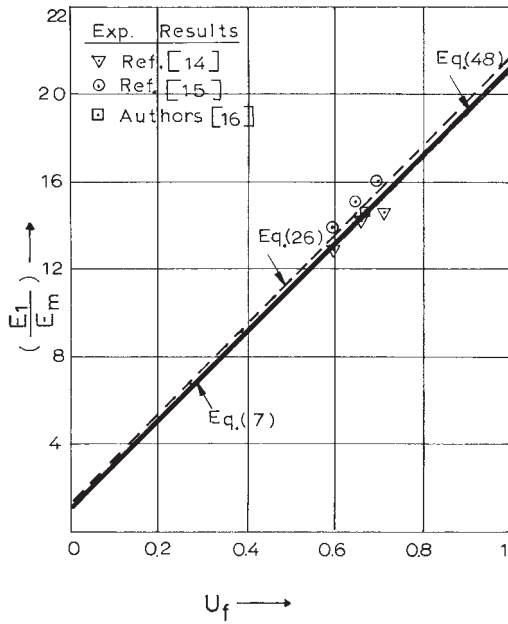
Figure 9 Variation of E_1 versus filler volume fraction.

It is known that a perfect bond between fibers is implied if a tensile σ_2 is applied, whereas no such bond is implied if a compressive σ_2 is applied. Also, more than 50% by volume of fibers is required to raise the transverse modulus E_2 to twice the matrix modulus. This means that the fibers do not contribute much to the transverse modulus unless the fiber volume fraction is very high. Obviously, the assumptions involved in the foregoing derivation are not entirely consistent. There is a transverse strain mismatch at the boundary, mainly between the fiber and interphase and also between matrix and interphase by virtue of eq. (8). Moreover, the transverse stresses in the fiber, the interphase, and in the matrix are not likely to be the same. Rather, a complete match of displacements across the boundaries fiber–interphase and interphase–matrix would constitute a rigorous solution to determine the apparent transverse elastic modulus. Such a solution can be accomplished only by use of the theory of elasticity.

Another observation on this solution is that, because of the difference in the Poisson's ratios of the fiber, the interphase and the matrix longitudinal stresses are induced in the three phases (with a net resultant longitudinal force of zero), with accompanying shearing stresses at the fiber–interphase and interphase–matrix boundaries. Such shearing stresses will naturally arise under some stress states. Thus, this material characteristic cannot be regarded as desirable or indicative of an appropriate solution. In the same figure, indicated by the dashed line, the theoretical values derived by Eckvall[10] and given in eqs. (27) and (28) are shown. These values are above those given by the developed theoretical model for $v_f < 0.8$.
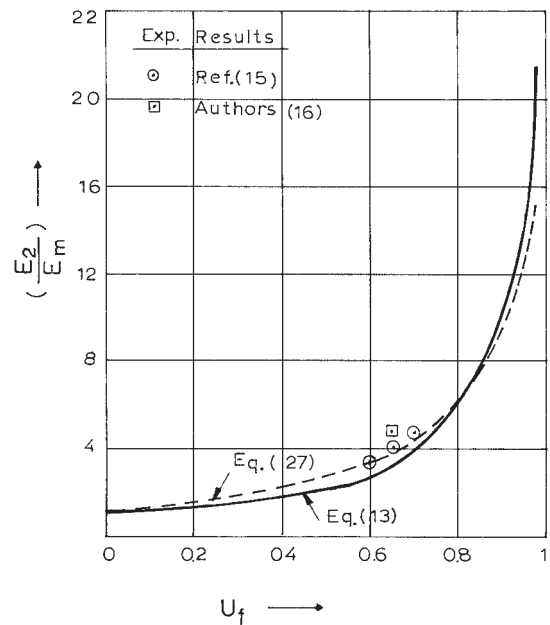
In the same figure, designated by the dashed line, the theoretical values derived by Eckvall[10] and given in eqs. (26) and (28) are shown. These values are slightly above those given by the developed theoretical model.

The experimental results show a slight discrepancy with theoretical values; that is, those given in Whitney and Riley[14] are below the theoretical values derived by the developed theoretical model, whereas those given in Clements and Moore[15] are above the theoretical values. It can be said that the coincidence is satisfactory.

In Figure 10 the variation of the elastic modulus in the direction transverse to the fibers E_2, as calculated through eq. (13) normalized by E_m, is presented. For $v_f = 1$ the modulus predicted is that of fibers. The values obtained from eq. (13) are superior to those given by the theoretical expression, which does not take into account the interphase (inverse mixtures law), because the interphase modulus E_i, calculated by eqs. (61) and (62), is greater than the matrix modulus E_m and because $v_i = 1 - v_f - v_m$. Thus

$$\frac{E_2}{E_m} = \frac{E_f}{(E_m v_f + E_f v_m) + \frac{E_f E_m}{E_i}(1 - v_f - v_m)}$$

which is greater than that given by the inverse mixture law

$$\frac{E_2}{E_m} = \frac{E_f}{E_m v_f + E_f v_m}$$

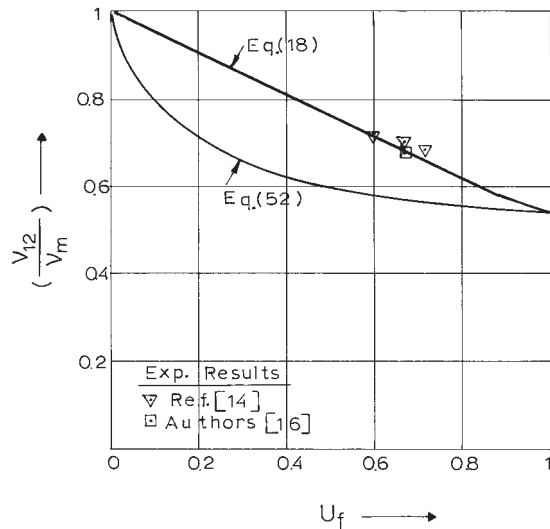**Figure 10** Variation of E_2 versus filler volume fraction.

Figure 11 Variation of ν_{12} versus filler volume fraction.

The experimental results given in Clements and Moore[15] show some discrepancy with the theoretical values derived by the developed theoretical model, although they are in very good agreement with those derived by Eckvall.[10]

Figure 11 presents the variation of the major Poisson ratio ν_{12}, as calculated from eq. (18), normalized by ν_m. This variation is analogous to that given by the mixtures law. However, the values obtained from eq. (18) are inferior to those given by the law of mixtures because the interphase Poisson ratio ν_i, calculated by eqs. (61) and (62), is less than the matrix Poisson ratio ν_m and because $\nu_i = 1 - \nu_f - \nu_m$. Thus

$$\nu_{12} = \nu_f \nu_f + \nu_m \nu_m - \nu_i(\nu_f + \nu_m) + \nu_i$$

which is less than that given by the mixture law $\nu_{12} = \nu_f \nu_f + \nu_m \nu_m$.

In the same figure the experimental results given in Whitney and Riley[14] are shown. These values are in good agreement with those derived from the developed theoretical model.

In Figure 12 the variation of the in-plane shear modulus G_{12}, as calculated from eq. (25) and normalized by G_m, is presented.

As in the case of E_2 the matrix modulus is the dominant term in this expression. Only for a fiber volume near 50% of the total volume does G_{12} rise above twice G_m. This variation is again analogous to that given by the mixtures law. However, the values obtained from eq. (25) are superior to those given by the theoretical expression, which does not take into account the interphase (inverse mixtures law), because the interphase modulus G_i, calculated by eqs. (61) and (62), is greater than the matrix modulus G_m and because $\nu_i = 1 - \nu_m - \nu_f$. Thus

$$\frac{G_{12}}{G_m} = \frac{G_f}{(G_m \nu_f + G_f \nu_m) + \dfrac{G_f G_m}{G_i}(1 - \nu_f - \nu_m)}$$

which is greater than that given by the inverse mixtures law

$$\frac{G_{12}}{G_m} = \frac{G_f}{G_m \nu_f + G_f \nu_m}$$

In the same figure the experimental results given in Clements and Moore[15] are shown. These values do not show agreement with those derived from the developed theoretical model. This formula seems to show the greatest degree of discrepancy with experiments.

In Figure 11 is also included the variation of the Poisson ratio ν, as calculated from eq. (52), normalized by ν_m. As can be seen the values of Poisson ratio, as derived by this expression, are well below the values given by eq. (18). This confirms that the expression of eq. (52) corresponds to a minimum for the Poisson ratio of the composite, as stated earlier in the theoretical analysis.

On the contrary, if these values of Poisson ratio ν are substituted in eq. (48) the values obtained are slightly greater than those obtained from eq. (7). This confirms that the expression of eq. (48) indeed constitutes an upper bound for the elastic modulus of the composite material, as stated earlier in the theoretical analysis.
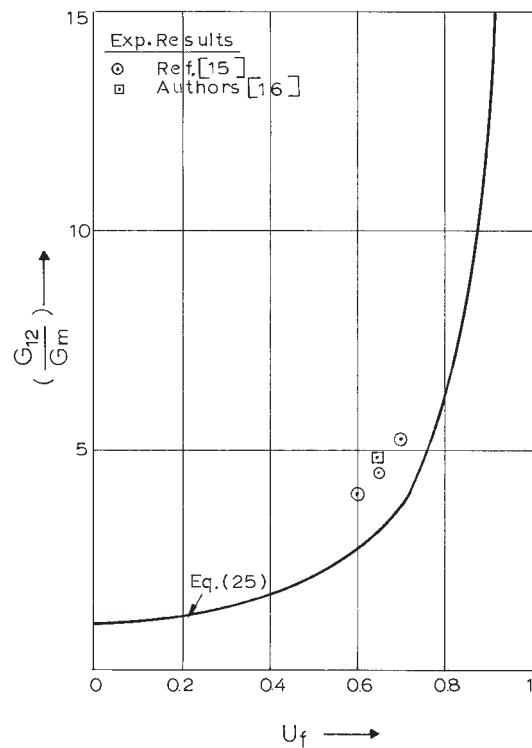

Figure 12 Variation of G_{12} versus filler volume fraction.

CONCLUSIONS

The concept of boundary interphase between the fibers and the matrix was used to obtain expressions for the longitudinal and transverse elastic moduli E_1 and E_2, the longitudinal Poisson ratio ν_{12}, and the in-plane shear modulus G_{12} of the composite material, using a strength of materials approach. The values obtained show some discrepancy compared with those obtained from the mixtures law or transverse mixtures law, which does not take the interphase into account. Also, using an elasticity approach bounds for the elastic modulus and Poisson ratio of the composite were found once again by taking the interface into account. The values obtained present a slight difference with those obtained from the theoretical expressions that do not take the interphase into account.

The experimental results are in very good agreement with the theoretical values derived from the developed model in the case of the longitudinal elastic modulus and Poisson ratio. However, they are not in good agreement with those for the transverse elastic modulus and show substantial discrepancy with those for the shear modulus.

References

1. Jones, R. M. Mechanics of Composite Materials; McGraw-Hill International Student Edition: New York, 1975.
2. Chamis, C. C.; Sendeckyj, G. P. J Compos Mater 1968, July, 332.
3. Hashin, Z. J Appl Mech 1962, March, 143.
4. Theocaris, P. S.; Sideridis, E.; Papanicolaou, G. C. J Reinf Plast Compos 1985, 4, 396.
5. Mikata, Y.; Taya, M. J Compos Mater 1985, 19, 554.
6. Pagano, N. J.; Tandon, G. P. Compos Sci Technol 1988, 31, 273.
7. Benveniste, Y.; Dvorak, G. J.; Chen, T. Mech Mater 1989, 7, 305.
8. Steif, P.; Dollar, A. J Appl Mech 1988, 55, 618.
9. Achenbach, J. D.; Zhu, H. J Appl Mech 1990, 57, 956.
10. Ekvall, J. C. In Structural Behaviour of Monofilament Composites, Proceedings of the 6th AIAA Conference on Structures and Materials; American Institute of Aeronautics and Astronautics: New York, 1965.
11. Paul, B. In Prediction of Elastic Constants of Multiphase Materials, Transactions of the Metallurgical Society of AIME, February 1960; American Institute of Mining, Metallurgical, and Petroleum Engineers: New York, p. 36.
12. Lipatov, Y. S. Physical Chemistry of Filled Polymers; originally published by Khimiya: Moscow, 1977 (in Russian); Moseley, R. J., Trans.; Int Polym Sci Technol Monogr 2.
13. Theocaris, P. S. In The Interphase and Its Influence on the Mechanical Properties of Composites: New Developments in the Characterization of Polymers in the Solid State; Kausch, H. H.; Zachmann, H. C., Eds.; Advances in Polymer Science; Springer-Verlag: New York, 1984.
14. Whitney, J. M.; Riley, M. B. AIAA J 1966, 4, 1537.
15. Clements, L. L.; Moore, R. L. Composites 1978, 1, 93.
16. Papadopoulos, G. A.; Sideridis, E. Arch Appl Mech 1995, 66, 111.